JOURNAL OF MATERIALS SCIENCE 29 (1994) 3161–3166

# New ternary nitride ceramics: $CaSiN_2$

W. A. GROEN, M. J. KRAAN, G. DE WITH
*Philips Research Laboratories, P.O. Box 80000, 5600 JA, Eindhoven, The Netherlands*

The synthesis of $CaSiN_2$ powder, starting from metal nitrides, is described. Fully dense $CaSiN_2$ ceramics can be sintered from the prepared powder at 1700 °C. The samples were sintered in a closed Mo vessel to prevent evaporation of calcium nitride. The phase composition, and the chemical and mechanical properties of the as-prepared ceramics are described. The thermal conductivity at room temperature was evaluated as 2.4 $W m^{-1} K^{-1}$. A reasonable strength of 179 MPa and a fairly good fracture toughness of about 2.1 $MPa m^{1/2}$ were found. A hardness of 9.6 GPa and a Young's modulus of 174 GPa were measured. The value of the relative dielectric constant was measured as 13.3. The bandgap for $CaSiN_2$ at room temperature was estimated from diffuse-reflectance spectra to be 4.5 eV. Considerable improvement in the properties are expected when the processing conditions which is well within reach are optimized.

## 1. Introduction

Interest has recently focused on nitride ceramics because they combine high thermal conductivity with high electrical resistance at room temperature. As discussed by Slack [1], there are only a few materials with a high electrical resistance at room temperature and a thermal conductivity at ambient temperatures which is in excess of 1 $W m^{-1} K^{-1}$. Most of these materials are compounds which crystallize in a diamond-like structure, for example BeO, SiC and AlN. In all of these structures the atoms are tetrahedrally coordinated. In these compounds, the heat flow is primarily carried by phonons. As a result, the thermal conductivity of these materials is largely dependent on impurities due to phonon scattering.

In addition to the binary compounds noted above, a number of ternary compounds also crystallize in a diamond-like structure. $BeSiN_2$ and $MgSiN_2$ crystallize in an orthorhombic structure, which is derived from the Wurtzite structure [2, 3]. The hexagonal structure is distorted because of the presence of two metal atoms and because of displacement of the nitrogen atoms from their ideal positions in the Wurtzite structure. $^{15}N$-nuclear magnetic resonance (NMR) experiments on a $^{15}N$-enriched $MgSiN_2$ sample indicated a complete ordering of the Mg and Si atoms [4]. The bandgap for $MgSiN_2$ is reported to be 4.8 eV when calculated from diffuse-reflectance spectra [5]. Recently, we reported a preparation of fully dense $MgSiN_2$ ceramics [6]. The thermal conductivity of these samples at room temperature has been estimated as 17 $W m^{-1} K^{-1}$. A reasonable strength of 270 MPa and a fairly good fracture toughness of about 4.3 $MPa m^{1/2}$ were obtained. A hardness of about 15 GPa and a Young's modulus of 235 GPa were measured. These data indicate that $MgSiN_2$ ceramics have promise as heat-sink materials if the thermal conductivity can be increased further.

These promising results for $MgSiN_2$ indicate that it could be worthwhile to investigate other ternary nitrides. An obvious choice is $CaSiN_2$. The crystal structure of $CaSiN_2$ is still unknown, but is probably related to a diamond-like structure. In this paper we present the preparation of a $CaSiN_2$ powder and ceramics starting from the binary nitrides. The phase composition, thermal stability, microstructure and mechanical properties of the as-prepared ceramics are reported. An investigation of the phase system Ca–Si–N was first reported by Laurent [7]. Three ternary phases were observed: $CaSiN_2$, $Ca_5Si_2N_6$ and $Ca_4SiN_4$. For $CaSiN_2$ (a grey powder) only the *d*-values, as observed from a Debye–Scherrer diagram, were reported. The density had been measured to be 3030 $kg m^{-3}$. Thermal decomposition of $CaSiN_2$ is reported to start at 1300 °C due to the high vapour pressure of Ca. Pugar et al. [8] described a new phase with about 80% purity for a phase using a 1:1 calcium–nitride:silicon–nitride starting mixture. This phase crystallizes in a face-centred-cubic lattice with a lattice constant of 1.4864 nm. Cubic face centring has been confirmed by electron diffraction. The crystal structure is reported not to be isotypic with any known mineral oxide [8].

## 2. Experimental procedure

The synthesis of the $CaSiN_2$ powder was performed starting from $Ca_3N_2$ (Cerac, 99.9%) and amorphous $Si_3N_4$ (Sylvania, SN402). A stoichiometric mixture of the powders was mixed in an agate mortar. This mixture was loaded into an alumina crucible, which was placed in a stainless-steel tube. The stainless-steel tube was sealed mechanically to prevent the evaporation of $Ca_3N_2$. The tube was subsequently fired in a nitrogen flow, for 16 h at 1250 °C, to prevent corrosion of the container. To minimize oxygen contamination,

0022–2461  

the handling of the starting materials was performed in an argon-filled glovebox. The resulting powder was milled using an agate ball mill in hexane for 24 h. The particle-size distribution of the as-prepared and of the milled powder was measured with a Shimadzu SA-CP4 centrifugal particle-size analyser.

From the resulting powder mixture, pellets were pressed (diameter $\approx 30$ mm, thickness $\approx 4$–6 mm) using a PMMA (polymethylmethacrylate) die at 5 MPa. These pellets were subsequently cold-isostatically-pressed at 200 MPa. The resulting relative density of the green compacts was $\sim 50\%$. The pellets were placed in a molybdenum vessel which was closed using arc welding in an argon ambient at a pressure $2 \times 10^4$ Pa. The vessel was heated in a hydrogen/nitrogen ambient (7% $H_2$) in a horizontal tube furnace. The heating rate was 20 °C $min^{-1}$ to the set point of 1700 °C. The sample was kept at this temperature for 5 h and it was cooled to room temperature at a rate of 3 °C $min^{-1}$.

Phase identification was carried out by means of X-ray diffraction (XRD) analysis (Philips PW1800 diffractometer) using monochromatized Cu–$K_\alpha$ radiation. For elemental analysis, a ceramic sample was dissolved in a $Na_2CO_3$ melt. Calcium and silicon were analysed using inductively coupled plasma-emission spectroscopy (ICP) after dissolving the melt in diluted HCl. The oxygen and nitrogen content was measured using a Leco TC 436 $O_2/N_2$ analyser.

Differential thermal analysis (DTA) was performed in order to investigate phase transformations and the thermal-resistance-to-oxidation of the powder. The measurements were performed using a home-built apparatus with a twin-thermocouple configuration, in dry flowing air at ambient pressure.

The density, $d$, of the samples was determined by the Archimedes method. The longitudinal wave velocity, $v_l$, and the shear wave velocity, $v_S$, were measured at 10 and 20 MHz, respectively, using the pulse-echo method. From $d$, $v_l$ and $v_s$, the Young's modulus, $E$, and the Poisson's ratio $\nu$, were calculated with the usual formula for isotropic materials. No correction for damping was applied since the loss tangent was less than 0.05 [9]. The standard deviation in the Young's modulus was estimated to be about 2 GPa.

The Vickers hardness, $H_V$, was measured on a polished specimen. A load of 20 N was applied for about 15 s. The average sample standard deviation, using five readings, was about 1.6 GPa.

The fracture toughness, $K_{Ic}$, was measured in a dry $N_2$ gas atmosphere ( $\sim$ 200 p.p.m. V $H_2O$) (dew point: $-36$ °C) with a three-point-bend test, (span 12 mm, crosshead spread 10 mm $min^{-1}$) using a specimen measuring $1 \times 3 \times 15$ $mm^3$. A notch with a relative depth of about 0.15 and a width of 100 μm was sawn into the specimen. Precracking was a Knoop indentation (10 N load) at the notch root on both sides of the specimen. The compliance factor was calculated as described in [10]. Small specimens make efficient use of the available material while retaining reliability and accuracy [11]. Five specimens were used for the $K_{Ic}$ determination, resulting in an average sample standard deviation of 0.1 MPa $m^{1/2}$. The strength was measured in the same bending set-up. Samples were sawn with a 100 μm diamond wheel. Seven specimens were used, resulting in a sample standard deviation of 20 MPa.

Thermal-diffusivity measurements were carried out using a photoflash method, which is described in detail by Söllter and Güther [12]. The thermal-expansion coefficient was determined in $N_2$ in the temperature range from 20–600 °C using a 1 cm long specimen in a dual-rod dilatometer (Netsch). As a reference, a fused silica sample with an expansion coefficient of $0.55 \times 10^{-6}$ $K^{-1}$ was used.

The bandgap for $CaSiN_2$ at room temperature was estimated from diffuse-reflectance spectra.

## 3. Results

The reacted powder was white. XRD results indicated that the powder is nearly single-phased $CaSiN_2$. The XRD pattern of the powder is presented in Fig. 1. For the purposes of comparison, the pattern according to [8] is also presented in Fig. 1c. The other phases which were observed are unidentified. Due to the presence of these phases, all attempts to solve the crystal structure using X-ray powder diffraction are as yet unsuccessful. The unit-cell parameters are presented in Table I. In order to allow comparison, previously reported unit-cell data are also given [8].

The results of the analysis of the oxygen and nitrogen contents are presented in Table II. The relatively large amount of oxygen found can be attributed to oxygen contamination in the amorphous $Si_3N_4$ which was used.

To ascertain that no significant amount of oxygen was incorporated in the crystal structure, which would result in a superstructure, some $CaSiN_2$ powder was prepared from high-purity crystalline $Si_3N_4$ powder (Cerac, 99.9%). No change was observed in the XRD pattern, indicating a similar crystal structure to oxygen-rich $CaSiN_2$. No fully dense ceramics could be prepared from this powder, probably due to the broad range in particle sizes and a relatively large particle size.

DTA measurements performed on the powder showed no signal at temperatures up to 750 °C. This demonstrates that no phase transitions occur in the crystal structure. Starting from 750 °C, a large signal was observed, this originated from the oxidation of the sample.

Particle-size analyses of the powder dispersed in ethanol showed the existence of relatively large particles ( $> 6$ μm). The powder was therefore milled for 24 h in hexane to obtain a narrower range in the particle-size distribution. SEM micrographs of the prepared powder, showing agglomerates of $CaSiN_2$ particles, are shown in Fig. 2. The particle-size distribution after milling are presented in Fig. 3.

The ceramic samples prepared from the milled powder had a light grey colour. The density of the pellets varied between 3030 and 3080 kg $m^{-3}$. The theoretical density can be calculated as 3137 kg $m^{-3}$ using the reported cell parameters [8] and the number of atoms per unit cell $Z = 64$, indicating that nearly full density has been achieved (96.5–98.2%). The XRD

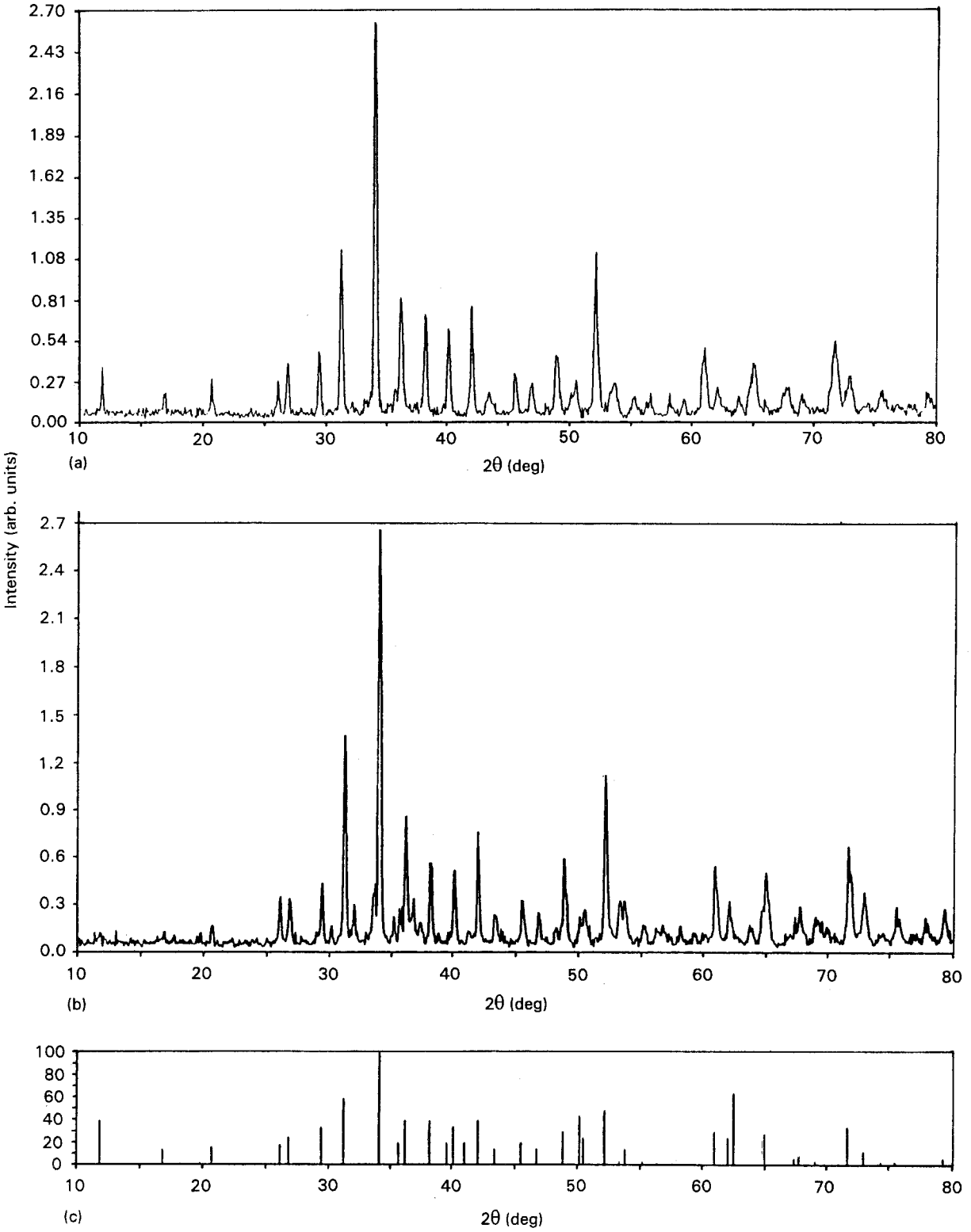


*Figure 1* The XRD patterns of (a) the $CaSiN_2$ powder, (b) the ceramic $CaSiN_2$ sample, and (c) the pattern according to [8].

TABLE I Unit-cell parameters of $CaSiN_2$ powder and ceramics, literature data are included

| Sample | $a$(nm) | Volume ($\times 10^{-30}$ m$^3$) |
|---|---|---|
| $CaSiN_2$ [8] | 1.4864 | 3284.0 |
| As-prepared powder | 1.4869 | 3287.3 |
| Ceramics | 1.4895 | 3304.6 |

TABLE II Compositions of the powder and ceramics (standard deviation is given in parentheses)

| Element | Powder (wt%) | Ceramic sample (wt%) | Theoretical (wt%) |
|---|---|---|---|
| Ca | – | 42(2) | 41.7 |
| Si | – | 28(1) | 29.2 |
| N | 25(1) | 22(1) | 29.1 |
| O | 5.4(0.3) | 7.1(0.3) | 0 |

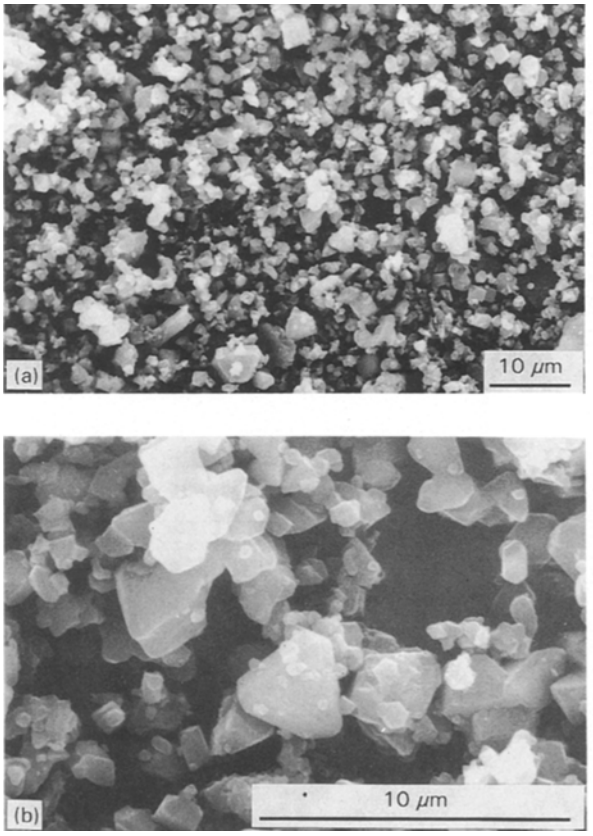


*Figure 2* SEM micrographs at two magnifications of the unmilled as-prepared powder, showing agglomerates of $CaSiN_2$ particles.

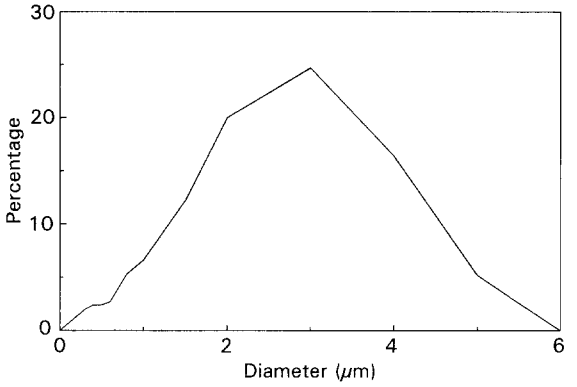


*Figure 3* The particle-size distribution of the $CaSiN_2$ powder after 24 h milling in hexane. The median diameter is 1.91 μm and the modal diameter is 2.34 μm.

pattern of a ceramic sample is also presented in Fig. 1. The lattice constants are given in Table I. The other phases observed in the sample are mainly $Ca_3Si_2O_4N_2$ [13]. The results of the analysis of the metal, oxygen and nitrogen contents are presented in Table II. The oxygen content of the ceramic sample was slightly higher than that of the powder. Presumably some oxidation or moisture pick-up occurred during handling.

The grain sizes and the morphology of the second phases of the sintered samples was examined by scanning electron microscopy (SEM). Fig. 4 shows SEM micrographs of a fractured sintered sample at different magnifications. The micrographs indicate that nearly full density had been achieved, but they also show a substantial amount of secondary phases. Large crystals were sometimes observed; they possibly consist of $Ca_3Si_2O_4N_2$ [13].

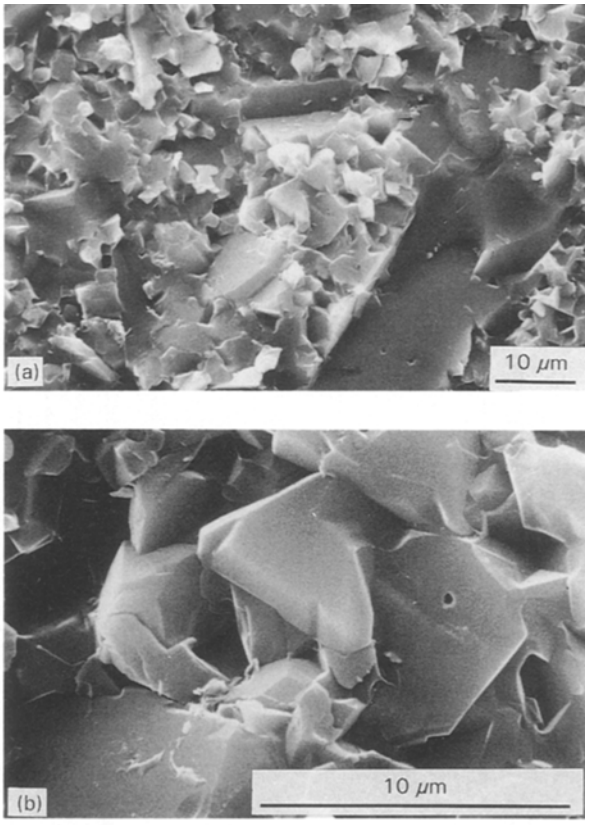


*Figure 4* SEM micrographs at two magnifications of the fracture surface of the sintered ceramic $CaSiN_2$ sample.

In order to obtain more detailed information about the microstructure, some of the pellets were polished and etched. SEM micrographs for a sample which was etched for 20 s in a 1% HF solution in water are shown in Fig. 5. The micrographs still show some porosity.

Measurements of the thermal diffusivity, $l$, on four samples resulted in an average value of 1.06(6) $mm^2 s^{-1}$. The thermal conductivity, $k$, can be estimated from this value using

$$k = l d C_p$$

Using the known $C_p$ value, where $C_p$ denotes the heat capacity, for AlN of 738 $J kg^{-1} K^{-1}$ [14] and the measured density, $d$, the thermal conductivity was estimated to be 2.4(0.1) $W m^{-1} K^{-1}$. The results for the measurements of the hardness, $H_V$, the fracture toughness, $K_{Ic}$, and the strength, are presented in Table III. For purposes of comparison, the reported mechanical properties of $Al_2O_3$, AlN and $MgSiN_2$ are also presented. The elastic properties are presented in Table IV. Again, literature data for $Al_2O_3$, AlN and $MgSiN_2$ are also included.

The relative dielectric constant, $\varepsilon_r$, was measured on a ceramic sample at room temperature using an *LCR* meter (HP4275A). On both sides of the sample a thin ( ~ 250 nm) silver layer was deposited by sputtering. The measurements were performed between 10 kHz and 10 MHz. The value of the relative dielectric constant was measured as 13.3 at 10 MHz. This value is slightly higher than the value for AlN [15] (9.1) and

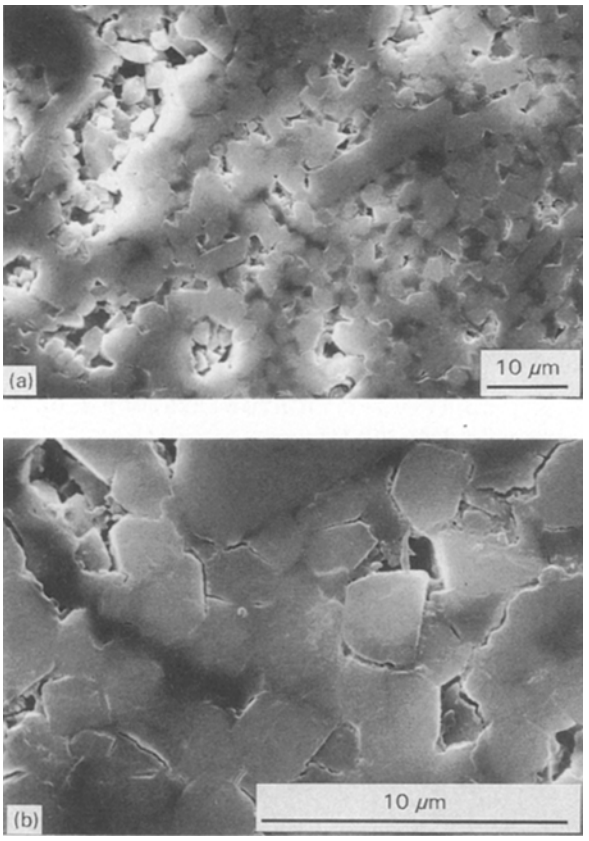


*Figure 5* SEM micrographs of a $CaSiN_2$ ceramic sample which was etched for 20 s in an aqueous solution of 1% HF.

TABLE III Mechanical properties of $CaSiN_2$ ceramics (the standard deviation and the number of measurements used are given in parentheses; and the properties for $MgSiN_2$, AlN and $Al_2O_3$ are also presented for comparison)

| Sample | $H_v$ (GPa) | $K_{Ic}$ (MPa $m^{1/2}$) | σ (MPa) |
|---|---|---|---|
| $CaSiN_2$ | 9.6(0.2, 5) | 2.1(0.1, 5) | 179(13, 7) |
| $MgSiN_2$ | 14.2[6] | 4.363[6] | 276[6] |
| AlN | 12[17] | 2.7[18] | 340[17] |
| $Al_2O_3$ | 19.5[19] | 4–5[19] | 450[17] |

for $MgSiN_2$ (10.5) [6]. The bandgap for $CaSiN_2$ at room temperature was calculated, from diffuse-reflectance spectra, to be 4.5 eV. The thermal expansion of a $CaSiN_2$ sample as a function of temperature was measured in $N_2$. The thermal-expansion coefficient, α, over the temperature range from 20–600 °C was measured to be $7.6 \times 10^{-6}$ $K^{-1}$.

## 4. Discussion

The value of the thermal conductivity, $k$, of 2.4 W $m^{-1}$ $K^{-1}$ is significantly lower than for $MgSiN_2$ ceramics (17 W $m^{-1}$ $K^{-1}$). This is expected to be due to the increased ionic character (calculated using Sanderson's model [16]) for $CaSiN_2$ (36%) compared with $MgSiN_2$ (32%). Also, the higher atomic weight of Ca compared to Mg will result in a lowering of the thermal conductivity. Finally, the differences in crystal structure between $CaSiN_2$ and $MgSiN_2$ may cause a difference in the thermal conductivity. Because of the presence of secondary phases as well as oxygen contamination, it is expected that the thermal conductivity can be increased considerably by optimizing the powder preparation and processing and by using better-quality precursor materials.

The hardness, fracture toughness and the strength measured for $CaSiN_2$ ceramics are all lower than those observed for $MgSiN_2$ ceramics. However, reasonable values are obtained compared to AlN. The value of Young's modulus, even corrected for porosity, is significantly lower than for $Al_2O_3$ and AlN. On the other hand, a relatively low value of Young's modulus has also been observed for $MgSiN_2$ [6].

The thermal-shock resistance of ceramics can be conveniently characterized by the parameters:

$$R = \sigma(1 - \nu)/E\alpha \quad (1)$$

$$R' = kR \quad (2)$$

where the variables have the meanings defined earlier. The parameter $R$ characterizes a material's resistance to thermal shock for high-heat-transfer conditions. The parameter $R'$ does the same, but for mild-heat-transfer conditions. From the experimental data, the parameters $R$ and $R'$ were calculated and they are given in Table IV. For the purpose of comparison, the values calculated for $MgSiN_2$, AlN and $Al_2O_3$ are also given. From Table IV it can be concluded that the thermal-shock-resistance parameter, $R$, for $CaSiN_2$ is comparable to that for $Al_2O_3$, but it is lower than for $MgSiN_2$ and AlN. However, due to the low thermal conductivity of $CaSiN_2$, the thermal-shock resistance for mild-heat-transfer conditions, $R'$ is significantly lower than for other ceramics.

## 5. Conclusions

In this paper, we have presented the preparation of a new ternary nitride ceramic, $CaSiN_2$. Nearly fully-dense material could be prepared by sintering in a

TABLE IV Elastic properties and the characteristic parameters, $R$ and $R'$, for the thermal-shock resistance of $CaSiN_2$ ceramics (the data for $MgSiN_2$, AlN and $Al_2O_3$ are also presented for comparison)

| Property | $CaSiN_2$ | $MgSiN_2$ | $Al_2O_3$ | AlN |
|---|---|---|---|---|
| σ (MPa) | 179 | 240–270[6] | 450 [17] | 340 [17] |
| $E$ (GPa) | 174 | 235 [6] | 398 [19] | 315 [20] |
| ν | 0.255 | 0.232 [6] | 0.235 [19] | 0.245 [19] |
| α ($\times 10^{-6}$ $K^{-1}$)[a] | 7.6 | 5.8 [6] | 7.9 [21] | 4.8 [21] |
| $k$ (W $m^{-1}$ $K^{-1}$) | 2.4 | 17 [6] | 20 [19] | 150 [22] |
| $R$ (K) | 100 | 130–150 | 110 | 170 |
| $R'$ (kW $m^{-1}$) | 0.24 | 2.2–2.5 | 2.2 | 25 |

[a] Measured between 20 and 600 °C.

closed Mo vessel. The thermal conductivity was estimated as 2.4 $W m^{-1} K^{-1}$. A reasonable strength of 179 MPa, a fairly good fracture toughness of 2.1 $MPa m^{1/2}$ and a hardness of 9.6 GPa were obtained, while a relatively low Young's modulus of 174 GPa was observed. The value of the relative dielectric constant was measured as 13.3. The bandgap for $CaSiN_2$ at room temperature was estimated from diffuse-reflectance spectra as 4.5 eV.

These data, together with those for $MgSiN_2$ [6], indicate that ternary nitride ceramics have promising properties which warrant further optimization.

## Acknowledgements

Thanks are due to J. Timmers for the X-ray analysis, to C. J. Geenen for the SEM work, to A. C. A. Jonkers for the elemental analyses, to N. A. M. Sweegers for the measurements of the mechanical properties and to H.-M. Güther (Hoechst A. G., Frankfurt am Main, Germany) for measurements of the thermal diffusivity.

## References

1. G. A.SLACK. *J. Phys. Chem. Solids* **34** (1973) 321.
2. P. ECKERLIN, *Z. Anorg. Allgem. Chem.* **352** (1967) 225.
3. J. DAVID, Y. LAURENT and J. LANG, *Bull. Soc. Fr. Mineral. Cristallogr.* **93** (1970) 153.
4. R. K. HARRIS, M. J. LEACH and D. P. THOMPSON, *Chem. Mater.* **4** (1992) 260.
5. G. K. GAIDO, G. P. DUBROVSKII and A. M. ZYKOV, *Neorg. Mater.* **10** (1974) 564.
6. W. A. GROEN, M. J. KRAAN and G. DE WITH, *J. Eur. Ceram. Soc.* in press.
7. Y. LAURENT, *Rev. Chim. Min.* **5** (1968) 1019.
8. E. A. PUGAR, J. H. KENNEDY, P. E. D. MORGAN and J. R. PORTER, *J. Amer. Ceram. Soc.* **71** (1988) C288.
9. H. F. POLLARD, "Sound waves in solids", (Pion Press, Amsterdam 1977).
10. W. F. BROWN and J. E. SRAWLEY, ASTM-STP-410 (American Society for Testing Materials, Philadelphia 1966).
11. G. DE WITH and N. HATTU, *J. Mater. Sci.* **16** (1981) 1702.
12. W. SÖLLTER and H.-M. GÜTHER, *Produktion und prüftechnik* **11** (1991) 106.
13. JCPDS card no. 38–944 (Joint Committee for Powder Diffraction Standards, Swathmore, Pennsylvania).
14. L. BARIN, O. KNACKE and O. KUBASCHEWSKI, "Thermochemical properties of inorganic substances", (Springer Verlag, Berlin, 1977).
15. A. T. COLLINS, E. C. LIGHTOWLERS and P. J. DEAD, *Phys. Rev.* **158** (1967) 833.
16. R. T. SANDERSON, *J. Chem. Educ.* **44** (1967) 516.
17. H. LANDOLT and R. BÖRNSTEIN, "Numerical data and functional relationships in science and technology", New Series, (Springer, Berlin 1980).
18. G. DE WITH and N. HATTU, *J. Mater. Sci.* **18** (1983) 503.
19. R. MORRELL, "Handbook of properties of technical and engineering ceramics, Part 2, data reviews" (Her Majesty's Stationary Office, London, 1987) p. 37.
20. P. BOCH, J. C. GLANDUS, J. JARRIGE, J. P. LECOMPTE and J. MEXMAIN, *Ceram. Int.* **8** (1982) 34.
21. Y. S. TOULOUKIAN, R. K. KIRBY and R. E. TAYLOR (Editors) "Thermophysical properties of matter" (Plenum, New York 1977).
22. C. KÖSTLER, H.-M. GÜTHER, H. BESTGEN, A. ROOSEN and W. BÖCKER, *2nd European Conference on Advanced Material Processes* Vol. 3 (The Institute of Materials, London, 1991) pp. 28–41.

*Received 2 August 1993*
*and accepted 10 January 1994*